

Real-time compression of high-bandwidth measurement data of thermographic cameras with high temporal and spatial resolution

by Z. Wang*, S. M. Najmabadi*, Y. Baroud*, M. Wachs**, G. Dammass** and S. Simon*

* University of Stuttgart, Universitaetsstr. 38, 70569 Stuttgart, Germany, zhe.wang@ipvs.uni-stuttgart.de

**InfraTec GmbH, Gostritzer Str., 01217 Dresden, Germany, {m.wachs, g.dammass}@infrotec.de

Abstract

The high temporal and spatial resolution of industrial thermographic cameras creates a rapid growth in the bandwidth of measurement data, such that the bandwidth of widely used standard data transmission links is becoming a performance bottleneck for thermographic systems. This paper proposes the use of real-time compression for the measurement data in future high-performance thermographic cameras. Real-time compression of high-throughput input stream is achieved via a lightweight and low-latency algorithm based on predictive coding. To obtain a high compression ratio while ensuring the quality of compressed data, the compression core exploits image-dependent measurement information such as calibration range and controls the compression quality correspondingly. Experimental results show that the proposed camera integrated thermographic data compression reduces the average required bandwidth by over 85%.

1. Introduction

Modern industrial thermographic cameras tend to provide high spatial and high temporal resolution. For example, thermographic image sequences taken by [1] have more than 1.3 Megapixels per frame with 14 bit per pixel at more than 100 frames per second (fps), resulting in a raw data rate of about 2Gbit/s. Such a bandwidth is beyond the capacity of the Gigabit Ethernet connection which is so far widely used for transmitting raw measurement data from thermographic cameras. Although the Camera Link standard provides up to 6Gbit/s bandwidth, it still imposes a limitation of performance e.g. in the case of a multi-sensor or multi-camera configuration and for future ultra-high resolution thermographic cameras. With the advances in infrared sensing technology continuously outpacing the increase in physical capacity/bandwidth of infrastructures, it is essential for future high-throughput thermographic systems to respond to the growing bandwidth challenge.

Compression of thermographic images has been considered in a number of works for reducing the amount of measurement data. Thermographic Signal Reconstruction (TSR) is a well-known method for analyzing thermographic image sequences based on curve fitting [2, 3]. In TSR the temperature at each pixel location is modeled as a polynomial in the logarithmic domain, such that significant compression can be achieved by storing only the collection of fitted parameters rather than the whole image sequence. Variants of the TSR-based method include e.g. using alternative fitting technique [4], using alternative heat transfer model [5], and classification of the original sequence into sub-sequences prior to TSR [6, 7]. By its nature, TSR assumes a cooling/heating process and a stationary object under test. Such assumptions are rarely met especially in passive thermography where no well-defined thermal diffusion process is available or when the object under test is moving e.g. due to operational requirements. The space/time mapping (STM) method [8, 9] transforms the input image sequence into a single image, which is then processed by a standard image compression algorithm like JPEG. Although originally designed for compressing the same type of data as those for TSR, STM does not necessarily require a diffusion process or a stationary object under test. While all these methods considerably reduce the amount of thermographic data, their computational complexity and memory requirement are significant given the high temporal and spatial resolution of modern thermographic cameras, since the whole image sequence needs to be stored and processed. Such methods hence result in a major challenge for a hardware/software implementation in real-time applications where the measurement data stream need to be compressed before being transmitted from the camera to an external host.

This paper focuses on online compression, which is an effective way to meet the growing bandwidth challenge at a reasonable cost. The term *online* compression is used in this paper to describe a compression taking place in real-time as the camera performs temperature measurements and before the transmission of the measurement data to a host PC, whereas the term *offline* compression is used for a compression after the camera finishes capturing a complete sequence of measurement data or after the transmission of the measurement data from the camera to a host PC. Because of the high computational and memory complexity, the TSR- and STM-based methods are suitable as offline compression schemes e.g. running on a PC for reducing the storage space for the measurement data.

The high-throughput nature of measurement data requires online processing which is lightweight and easy to implement in hardware e.g. FPGAs. FPGAs are reconfigurable computing devices which can be integrated onto the sensor chips. The inherent parallel computing capacity of an FPGA enables the simultaneous use of various signal processing algorithms e.g. fixed-pattern-noise cancellation and compression in a cost-efficient way.

In this paper we propose a real-time and low-complexity compression system for high-throughput measurement data stream of thermographic cameras with high temporal and spatial resolution. The remainder of this paper is organized as follows. Section 2 provides a review of standard image compression techniques and discusses their limitations when used for high-throughput thermographic image streams. The proposed real-time compression system is presented in Section 3. Compression results based on real thermographic images are presented in Section 4. Finally Section 5 concludes this paper.

2. Review of standard image compression schemes

Existing standard image compression techniques can be divided into two types: transform domain codecs and pixel domain codecs. Transform domain codecs such as JPEG [10], JPEG 2000 [11] and H.264 [12] are widely used in consumer digital cameras, digital cinema and video camcorders. The main algorithmic blocks of a transform domain codec include transformation of pixel blocks into target signal domain, quantization in the transform domain and entropy coding. Because of the properties of the transform basis such as energy compaction and the quantization step sizes chosen based on known properties of the human visual system, transform domain codecs can provide a relatively high compression factor e.g. 8-10 without creating obvious visual artifacts in the reconstructed image.

One of the problems of the transform domain codecs, however, is the possibility of locally large compression error in the measured temperature, i.e. pixel value in the thermographic image. Although the thermographic image compressed by a transform domain codec e.g. JPEG may show no obvious visual artifacts overall, the difference between the original image and the compressed image can still exceed the desired maximum error threshold in certain local regions such as edges. Due to the transform, there is no straightforward way to predict or control the amount or location of such local temperature differences in transform domain codecs, which can be undesirable in applications where the maximum compression error in the measurement data need to be strictly defined.

Another issue for transform domain codecs is the relatively high computational and memory complexity. Many high-throughput thermographic cameras are embedded systems facing constraints like hardware cost, latency and power consumption. Existing transform domain video compression standards like H.264 has both relatively high memory complexity due to the storage of reference frames and relatively high computational complexity which creates a significant challenge for an implementation to meet the bandwidth requirement for images with Megapixel-resolutions and a temporal resolution in the 100 fps range at a reasonable cost. Existing transform domain image compression standards such as JPEG and JPEG 2000 require storing multiple sample lines before compression, which results in a significant demand of expensive on-chip memories as well as an increased latency which is a disadvantage for instance in real-time industrial monitoring applications.

Pixel domain codecs are used e.g. in remote sensing and medical imaging. Pixel domain codecs are typically less computationally complex and more memory efficient than transform domain codecs. The main algorithmic parts of a pixel domain coded include prediction, pixel domain quantization and entropy coding. JPEG-LS [13] is the state-of-the-art standard algorithm for lossless and near-lossless image compression in pixel domain. Experimental results with medical thermographic images in [14] shows that JPEG-LS outperforms other pixel domain codecs like CALIC [15] and FELICS [16] in terms of compression factor and for lossless compression. Unfortunately, when used for lossless compression, pixel domain codecs like JPEG-LS have limited compression factor such as 1.5-2. In order to transmit a thermographic image stream e.g. of Full-HD resolution at 100 fps and 16 bit per pixel, an average compression factor of at least 3-6 is required for transmitting the measurement data using a standard Gigabit Ethernet interface in real-time.

The compression factor requirement can be met by using lossy compression with pixel domain codecs. In fact, lossy compression with a pixel domain codec potentially has an advantage over a transform domain codec in terms of measurement quality, since it is straightforward to control the amount of compression distortion to the measurement data via setting the quantization step size in a pixel domain codec. While the lossy mode of JPEG-LS can provide satisfactory compression factors, it is known that pixel domain codecs like JPEG-LS tend to produce visual artifacts in relatively smooth region of the image. Figure 1 shows an example. It can be seen that there are stripe-like artifacts in smooth part of the object. Such artifacts are caused by the pixel-wise processing nature in a raster scan order of the pixels and the quantization errors propagated from the previously encoded neighboring pixels. Such visual artifacts are undesirable since they may result in misinterpretation of the measurement data especially when a human inspector is involved. Due to such artifacts, the use of JPEG-LS for lossy compression is very limited.

Based on the above discussion, the set of requirements of a compression algorithm suitable for real-time high-throughput thermographic image sequence can be derived as follows.

- The algorithm should provide the possibility to directly control the compression distortion in the compressed measurement data.
- The algorithm should provide a compression factor higher than that of a lossless compression algorithm, such as 3-6.
- The algorithm should not result in apparent visual artifacts in the compressed image.
- The algorithm should have relatively small computational and memory complexity.

In the following section, we discuss how the proposed algorithm meets these requirements.

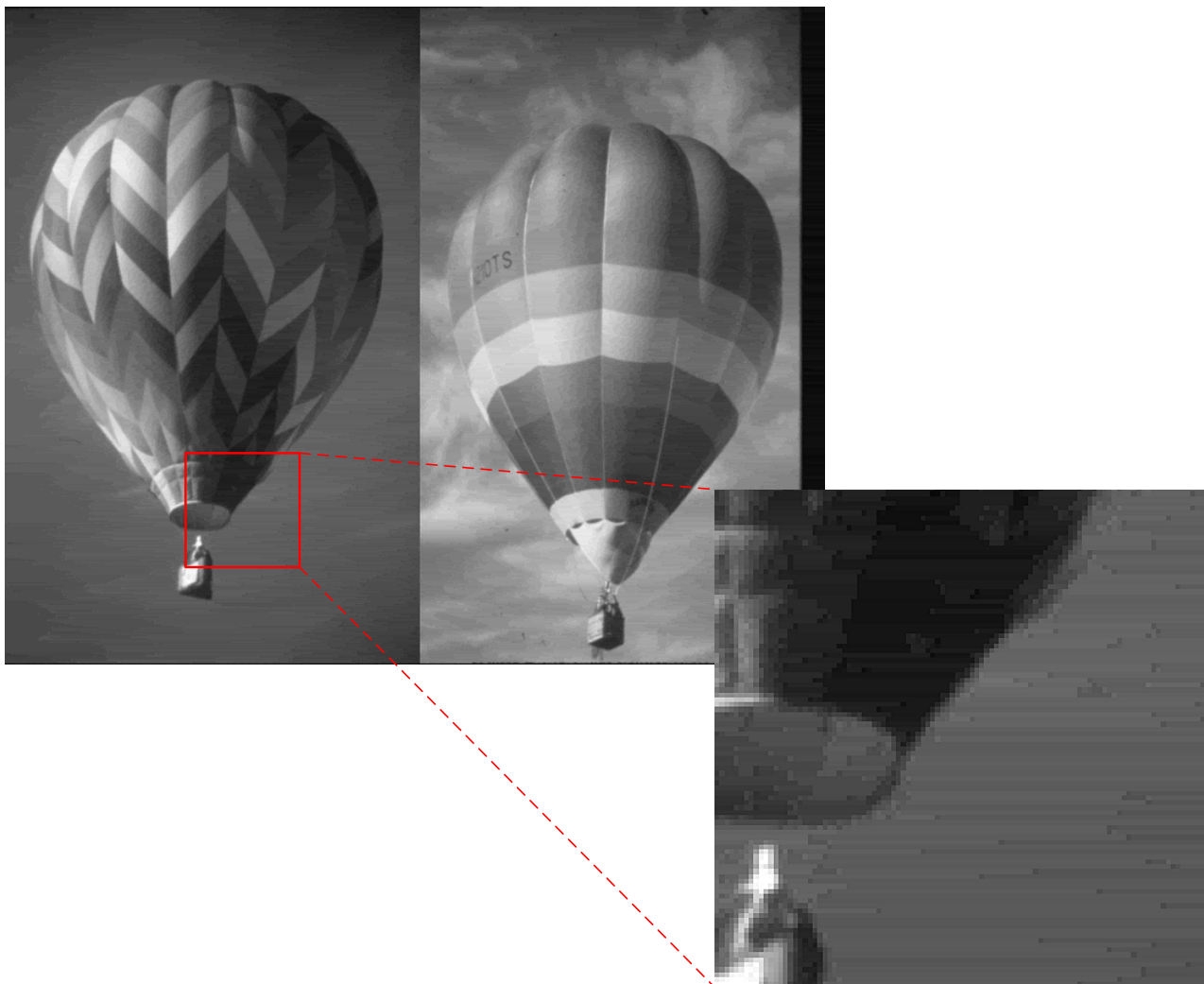


Fig. 1. Visual artifacts in the “balloon” image compressed by lossy JPEG-LS.

3. Camera integrated thermographic data compression system

The proposed thermographic data compression system process thermographic samples directly in the camera in real-time. The system is mainly composed of a sensor, an FPGA and a transmission interface, as shown in the top part of Figure 2. In a high performance camera, the infrared sensor measures temperature of the object under test at high temporal and spatial resolution, resulting in a large bandwidth of e.g. several Gigabits per second. The FPGA is a flexible reconfigurable computing device which is integrated into the camera and performs various data processing tasks in parallel, such as radiometric calibration for an improved quality of the measurement data as well as compression for an effective reduction of the bandwidth of the measurement data. The compressed measurement data have a reduced bandwidth of e.g. a few Megabits per second, which is feasible to be sent to an external host via standard on-camera data transmission interfaces such as Gigabit Ethernet or Camera Link.

Inside the FPGA, the compression core is located behind a pre-processing unit, as illustrated in Figure 2. The pre-processing unit carries out necessary steps such as Non-Uniformity-Correction (NUC) for achieving an acceptable image quality depending on the sensor or the application scenario. The outputs of the pre-processing unit are streams of measured digital values or pixels in the thermographic image. Such pixel streams are the inputs to the compression core. A data reduction block is used to adaptively decrease the amount of input samples based on whether the current subset of samples belong to a region-of-interest (ROI). The ROIs are identified by user-defined criteria such as a particular temperature range, local activity threshold, max error bound and so on. Other algorithmic parts of the compression core are based on the predictive coding principle similar to that in [13]. Here a prediction unit is used for the decorrelation of measurement data. A quantization unit for the restriction of sample bit-depth controls the quality of the compression based on sensor-/measurement-dependent information such as calibration range. And a hardware-efficient entropy coding unit generates the final compressed bitstream. In the following we present the key algorithmic parts.

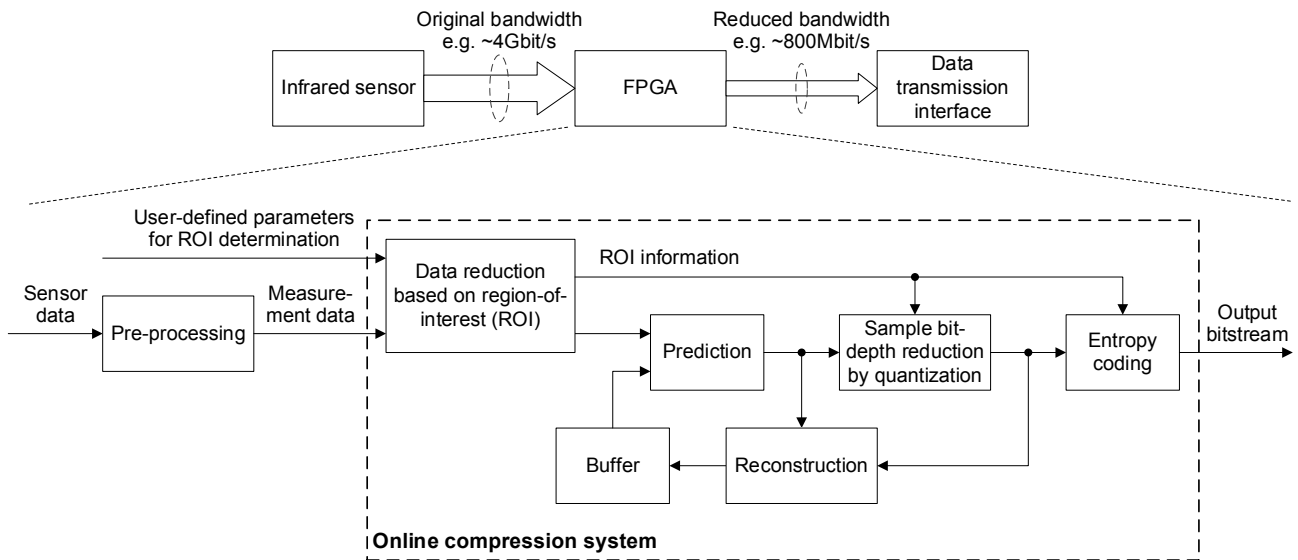


Fig. 2. Overview of the in-camera real-time thermographic data compression system.

3.1 Data reduction based on ROI

The main idea is that in general not all pixels in a thermographic image are equally important for a given application. For example, in medical imaging, only temperature in a particular range of e.g. 20-40 degree Celsius are relevant for the purpose of diagnosing human patients. Therefore temperature samples inside this range shall be compressed either with very small error or no error at all to maintain a high quality, whereas temperature samples outside this range can be compressed more heavily to gain compression efficiency. Another example is surface artifact detection, where local temperature variations above a particular threshold could indicate an artifact and shall hence be processed with high quality, while regions with little variations can be safely considered as artifact-free parts and can hence be more heavily compressed.

Based on the above observations, a flexible and robust ROI detection scheme is employed in the proposed algorithm. A subset of input samples S_1, S_2, \dots, S_n are examined against an application-specific condition defined by the user. If such conditions are met for the current subset, then the subset is considered as an ROI and a certain quality level (such as lossless), which can be again defined by the user, must be guaranteed for all samples in the subset. Otherwise, the subset is considered as a non-ROI. Such a condition is subsequently termed as an *ROI condition* in this paper. Note that since original data rather than compressed data are used for the ROI determination, the robustness of the detection scheme and hence the quality level of a compressed subset can be guaranteed given any ROI condition. The ROI information is also used in the quantization block to control the quality level of the compressed samples and is part of the output bitstream.

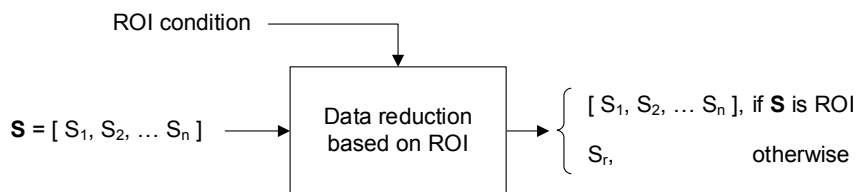


Fig. 3. Data reduction block.

Data reduction takes place when a subset, or pixel block, is non-ROI. In this case individual sample values in the subset can be considered as no longer important and it is hence feasible to reduce the amount of the sample values by calculating one or more representative values for the current subset e.g. via sub-sampling. The number of input samples is considerably decreased after the data reduction, for example by a factor of 6 if one representative pixel value is calculated per 6-pixel-block. As can be seen in Figure 3, the representative values undergo the normal predictive coding process, leading to further compression. While it is possible to apply high quantization on the representative

values for non-ROI subsets for an improved compression, non-ROI regions are empirically relatively smooth parts of the image where visual artifacts tend to occur for a pixel domain codec due to quantization error propagation. It is therefore reasonable to consider using either small quantization steps or no quantization at all for non-ROI regions, unless it is necessary to achieve a better compression performance e.g. due to the bandwidth constraint.

3.2 Prediction

Most imaging systems output pixel samples one after another in a line-wise manner. The proposed algorithm hence follows a raster scan encoding order, as shown in Figure 4. In this figure, i, j stand for spatial indices and x stands for the current sample value to be encoded. Note that because of the data reduction, the value of x is ROI-dependent. For example, let $S_{i,j}$ be the input pixel value at location (i, j) and let the current subset be composed of $S_{2,5}, S_{2,6}, S_{2,7}$, with S_r being the representative value for this subset, as depicted in Figure 4. If the current subset is ROI, then the value of x is $S_{2,5}$. Otherwise S_r is used at the value of x .

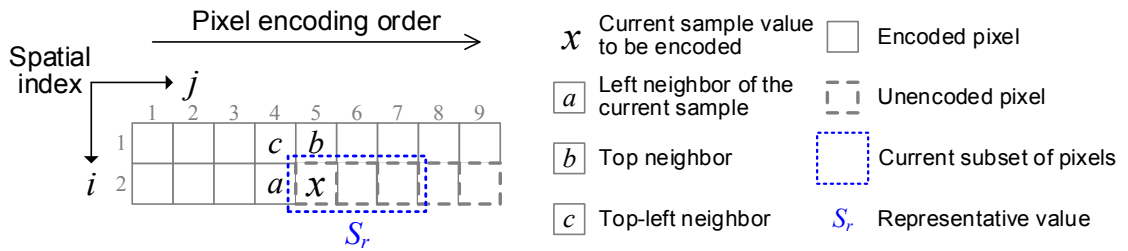


Fig. 4. Encoding order and prediction neighborhood for a current sample value.

For each sample value to be encoded, the proposed algorithm employs predictive coding, where a prediction of the current sample is calculated based on already encoded pixels in a causal neighborhood. Specifically, a so-called median edge detector (MED) from [13] is used in the proposed algorithm. Three encoded pixels a, b, c as illustrated in Figure 4 are the prediction neighborhood. The prediction P_x is given by the median of the three values a, b , and $a+b-c$, or equivalently,

$$P_x = \begin{cases} \min(a, b), & \text{if } c \geq \max(a, b) \\ \max(a, b), & \text{if } c \leq \min(a, b) \\ a + b - c, & \text{otherwise} \end{cases} \quad (1)$$

where $\min()$ and $\max()$ are the minimum and maximum operators respectively. Residual ε is then calculated as

$$\varepsilon = x - P_x, \text{ where } x = \begin{cases} S_{i,j}, & \text{if current subset is ROI} \\ S_r, & \text{otherwise} \end{cases} \quad (2)$$

After the prediction, the input sample values are converted into residual values, whose statistical redundancy can be better exploited by the entropy coder.

3.3 Sample Bit-depth Reduction by Quantization

Apart from the ROI-based data reduction and entropy coding, further compression can be achieved via reducing the bit-depth of the residual samples by quantization. In particular, when the current subset of pixels is an ROI, the number of samples is not decreased by the data reduction. This would mean only the statistical redundancy in the residual data can be exploited by the entropy coder, which would result in a very limited compression performance. In order to achieve improved compression performance on ROI parts of the image, bit-depth reduction of the residual samples by quantization can be used. Although the ROI pixels are more important than non-ROI pixels, a certain amount of compression distortion might still be affordable in practice, e.g. because of calibration noise in the input samples. The potential quality loss for ROI pixels, however, must be strictly controlled. This can be readily done via pixel-domain quantization. The proposed algorithm uses the quantizer from [13] with the additional feature that the quantization step size is adaptive to the ROI information. JPEG-LS defines a lossy coding parameter δ which is a bound for the maximum coding error. The quantization step size is given by $2\delta+1$, which is fixed for an encoding scan in JPEG-LS. Since in many thermographic images ROI pixels can be distinguished from non-ROI pixels, it is reasonable to set different maximum distortion bounds for ROI and non-ROI pixels, so that both significant compression and good quality can be achieved for a thermographic image. Let q_{ROI} and $q_{non-ROI}$ be the maximum acceptable compression distortions for ROI and non-ROI pixels, quantization in the proposed system is performed by:

$$Q(\varepsilon) = \text{sign}(\varepsilon) \cdot \left\lfloor \frac{|\varepsilon| + \delta}{2\delta + 1} \right\rfloor, \quad (3)$$

where

$$\delta = \begin{cases} q_{ROI}, & \text{if current subset is ROI,} \\ q_{non-ROI}, & \text{otherwise.} \end{cases} \quad (4)$$

Even in the case that only a universal quality level is desired for the compressed image, using an ROI-adaptive quantization step size can still be an advantage for the compression system, for example when visual artifacts tend to occur more often in certain types of regions of the compressed thermographic image than other types of regions.

4. Experimental results

The proposed compression system has been experimentally implemented in software and its compression performance has been tested using real thermographic images shown in Figure 5. Measurement data precision for all test images is 14bits/sample. Errors in the compressed images are limited to within 1% of the calibration range of respective images. Table 1 shows the respective resolutions for the test images, their sizes before and after compression in bytes and the compression ratio. It can be seen from the table that the compression ratio ranges between 3.0 and 10.4. On average a compression ratio of 6.7 has been achieved, leading to an average of 85% reduction in the required bandwidth for transmitting the measurement data.

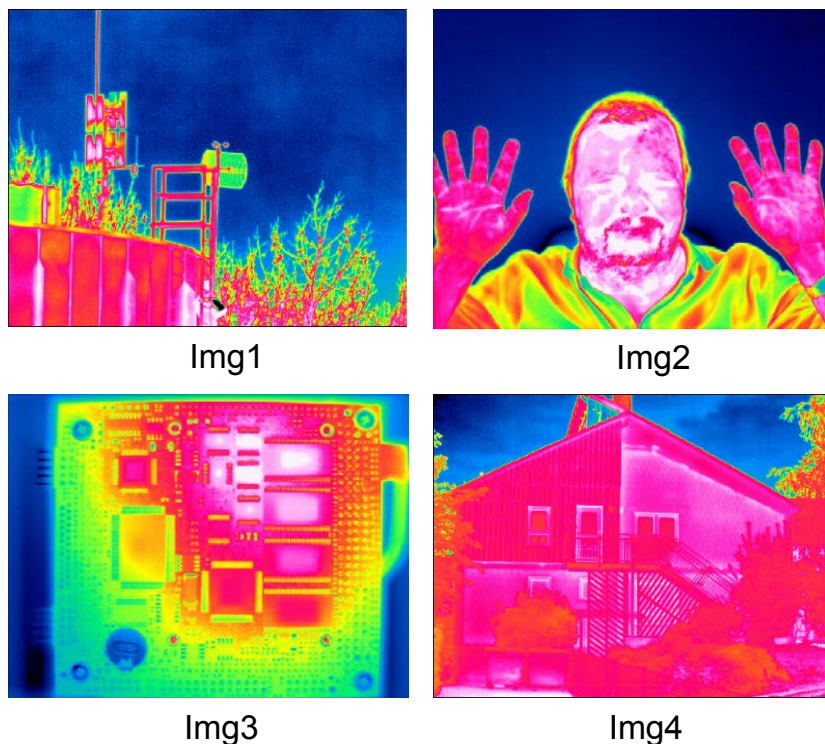


Fig. 5. Test thermographic images.

Table 1. Compression results of the proposed system.

| Test image | Resolution | Raw size [Bytes] | Compressed size [Bytes] | Compression ratio [-] |
|------------|------------|------------------|-------------------------|-----------------------|
| Img1 | 640x512 | 573,440 | 88,097 | 6.5 |
| Img2 | 1280x1024 | 2,293,760 | 220,051 | 10.4 |
| Img3 | 616x457 | 492,646 | 73,883 | 6.7 |
| Img4 | 1024x768 | 1,376,256 | 453,558 | 3.0 |
| Average | | | | 6.7 |

5. Conclusion

A real-time compression scheme has been proposed in this paper to address the growing bandwidth issue caused by high-throughput measurement data in modern thermographic cameras with high temporal and spatial resolutions. The algorithm makes efficient use of algorithmic tools in standard pixel domain predictive coding techniques and introduces a novel data reduction scheme exploiting sub-sampling and quantization adaptively based on the region-of-interest (ROI) determined in real-time for the input image. The ROI determination scheme is based on quality criteria defined by the user. The proposed ROI determination scheme is a general approach and is flexible to different application requirements such as important temperature range, local temperature variations and so on. Since the proposed algorithm works in the pixel domain, the amount of compression distortion in the reconstructed thermographic images can be accurately controlled by setting the quantization step size to the user-defined distortion threshold independently for ROI and non-ROI regions. Because of the lower computational and memory complexity compared with standard transform domain image compression techniques like JPEG 2000, the proposed algorithm is suitable for fast and cost-efficient implementation in hardware such as FPGAs. Experimental results based on a software implementation and real thermographic test images have shown an average compression factor of 6.7, leading to an average of 85% reduction in the required bandwidth for transmitting of the measurement data.

REFERENCES

- [1] InfraTec GmbH, "Infrared camera ImagerIR 9300 Series", Datasheet, Dresden, 2012.
- [2] S.M. Shepard, T. Ahmed, B.A. Rubadeux, D. Wang and J.R. Lhota, "Synthetic processing of pulsed thermographic data for inspection of turbine components," *Insight: Non-Destructive Testing and Conditioning Monitoring*, Vol. 43, No. 9, pp. 587-589, Sep. 2011.
- [3] S.M. Shepard, "Temporal noise reduction, compression and analysis of thermographic image data sequences," U.S. Patent 6 516 084, Feb. 4, 2003.
- [4] J. Zhang, X. Meng, W. Xu, W. Zhang and Y. Zhang, "Research on the compression algorithm of the infrared thermal image sequence based on differential evolution and double exponential decay model," *The Scientific World Journal*, Vol. 2014, 601506, Feb. 2014.
- [5] J.C. Ramirez-Granados, G. Paez, M. Strojnik, "Dimensionless heat transfer model to compress and analyze pulsed thermography data for NDT of materials," *Proc. SPIE 6939*, Thermosense XXX, 69391, Mar. 2008.
- [6] J. Zhang, W. Xu, W. Zhang, X. Meng and Y. Zhang, "A novel compression algorithm for infrared thermal image sequence based on K-means method," *Infrared Physics & Technology*, Vol. 64, pp. 18-25, May 2014.
- [7] J. Zhang, X. Meng, W. Zhang and S. Tao, "A novel algorithm for reconstruction of infrared thermographic sequences based on image segmentation," *Signal Processing, Communications and Computing (ICSPCC), 2014 IEEE International Conference on*, pp. 747-752, Guilin, Aug. 2014.
- [8] S. Lugin, U. Netzelmann, "An effective compression algorithm for pulsed thermography data," *NDT & E International*, Vol. 38, No. 6, pp. 485-490, Sep. 2005.
- [9] S. Lugin, U. Netzelmann, "Effective compression algorithms for pulsed thermography data," *Quantitative InfraRed Thermography Journal*, Vol. 3, No. 2, pp. 201-217, 2006.
- [10] *Information technology – Digital compression and coding of continuous-tone still images – Requirements and guidelines*, ISO/IEC 10918-1, Sep. 1992.
- [11] *Information technology – JPEG 2000 image coding system – Part 1: Core coding system*, ISO/IEC 15444-1, Dec. 2000.

- [12] *Information technology – Coding of audio-visual objects – Part 10: Advanced Video Coding*, ISO/IEC 14496-10, May 2003.
- [13] *Information technology – Lossless and near-lossless compression of continuous-tone still images: Baseline*, ISO/IEC 14495-1, Dec. 1999.
- [14] G. Schaefer, R. Starosolski and Shao Ying Zhu, "An evaluation of lossless compression algorithms for medical infrared images," *2005 IEEE Engineering in Medicine and Biology Society, 27th Annual Conference*, pp. 1673-1676, Shanghai, Sep. 2005.
- [15] X. Wu and N. Nemon, "Context-based, adaptive, lossless image coding," *IEEE Transactions on Communications*, Vol. 45, No. 4, pp. 437-444, Apr. 1997.
- [16] P. Howard and J. Vitter, "Fast and efficient lossless image compression," *1993 Data Compression Conference (DCC)*, pp. 351-360, Snowbird, Utah, Mar. 1993.